Effect of pseudogap on electronic anisotropy in the strain dependence of the superconducting T_c of underdoped $YBa_2Cu_3O_y$

M. Frachet,[1,*] Daniel J. Campbell,[1] Anne Missiaen,[1] S. Benhabib,[1] Francis Laliberté,[1] B. Borgnic,[1] T. Loew,[2] J. Porras,[2] S. Nakata,[2] B. Keimer,[2] M. Le Tacon,[3] Cyril Proust,[1] I. Paul,[4,†] and David LeBoeuf[1,‡]

[1]*LNCMI-EMFL, CNRS UPR3228, Université Grenoble Alpes, Université Toulouse, Université Toulouse 3, INSA-T, Grenoble and Toulouse, France*

[2]*Max-Planck-Institut für Festkörperforschung, Heisenbergstrasse 1, D-70569 Stuttgart, Germany*

[3]*Institute for Quantum Materials and Technologies, Karlsruhe Institute of Technology, D-76344 Eggenstein-Leopoldshafen, Germany*

[4]*Laboratoire Matériaux et Phénomènes Quantiques, CNRS, Université de Paris, F-75205 Paris, France*

(Received 1 June 2021; revised 10 November 2021; accepted 30 November 2021; published 4 January 2022)

For orthorhombic superconductors we define thermodynamic anisotropy $N \equiv dT_c/d\epsilon_{22} - dT_c/d\epsilon_{11}$ as the difference in how superconducting T_c varies with strains ϵ_{ii}, $i = (1, 2)$, along the in-plane directions. We study the hole doping (p) dependence of N on detwinned single crystals of underdoped $YBa_2Cu_3O_y$ (YBCO) using the ultrasound technique. While the structural orthorhombicity of YBCO reduces monotonically with decreasing doping over $0.065 < p < 0.16$, we find that the thermodynamic anisotropy shows an intriguing enhancement at the intermediate doping level, which is of electronic origin. Our theoretical analysis shows that the enhancement of the electronic anisotropy can be related to the pseudogap potential in the electronic spectrum that itself increases when the Mott insulating state is approached. Our results imply that the pseudogap is controlled by a local energy scale that can be tuned by varying the nearest-neighbor Cu-Cu bond length. Our work opens the possibility to strain engineer the pseudogap potential to enhance the superconducting T_c.

DOI: 10.1103/PhysRevB.105.045110

The link between electronic anisotropy and high-temperature superconductivity in the cuprates and the iron-based systems is a subject of great current interest. While a lot of progress on this topic has been made for the iron-based systems, relatively less is known about the in-plane electronic anisotropy observed in the pseudogap state of certain underdoped cuprates [1–12]. The microscopic factors governing this anisotropy are currently unknown, and are the subject of intense research [13–18]. Evidently, identifying the source of this anisotropy is of utmost importance for understanding the pseudogap state and the phase diagram of the cuprates. The purpose of the current joint experimental and theoretical study is to address this issue.

Experimentally, the anisotropy has been probed using a variety of techniques including in-plane electrical conductivity [1], torque magnetometry [2], neutron [3,4] and x-ray [5] diffraction, Nernst coefficient [6,7], scanning tunneling spectroscopy [8,9], nuclear magnetic resonance [10], and elastoresistivity [11]. One school of thought has identified the pseudogap temperature $T^\star$ with an electronic nematic phase transition [2]. However, the situation is unclear because signatures of diverging nematic correlation, expected near a nematic phase transition [19], have not been detected in the electronic Raman response in $Bi_2Sr_2CaCu_2O_{8+\delta}$ [20].

Motivated by the status quo, we study the doping evolution of the thermodynamic anisotropy $N \equiv dT_c/d\epsilon_{22} - dT_c/d\epsilon_{11}$, where $dT_c/d\epsilon_{ii}$ is the variation of the superconducting T_c with uniaxial strain ϵ_{ii}, $ii = (11, 22)$, of underdoped $YBa_2Cu_3O_y$ (YBCO). The experimental technique involves measuring the jumps in the associated elastic constants Δc_{ii} at T_c using sound velocity measurements (see Fig. 1), from which we extract $dT_c/d\epsilon_{ii}$ using the Ehrenfest relationship. The advantage of this method is that the strain dependence of T_c is obtained in *zero* applied static strain, as explained below. Consequently, the measurement is free of nonlinear effects that can be difficult to interpret.

This thermodynamic anisotropy is in line with earlier studies of uniaxial pressure dependencies of T_c [21,22]. However, converting them into strain dependencies is difficult due to the large uncertainties in the experimental values of the elastic constant tensor.

Our main observation is that, while the crystalline anisotropy, namely the orthorhombicity, reduces monotonically with decreasing hole doping over $0.065 < p < 0.16$ [23–25], the thermodynamic anisotropy $N(p)$ is a nonmonotonic function of p (see Fig. 2). In particular, in the range $0.11 < p < 0.14$, $N(p)$ does not track the orthorhombicity, but instead it increases when p is reduced. We therefore conclude that the observed nonmonotonic evolution is rooted in electronic effects. Our theoretical modeling suggests that the enhanced electronic anisotropy in this doping range is due to the pseudogap and its doping dependence. In other words, the

*Present address: Institute for Quantum Materials and Technologies, Karlsruhe Institute of Technology, D-76344 Eggenstein-Leopoldshafen, Germany.

†indranil.paul@univ-paris-diderot.fr

‡david.leboeuf@lncmi.cnrs.fr

 ©2022 American Physical Society

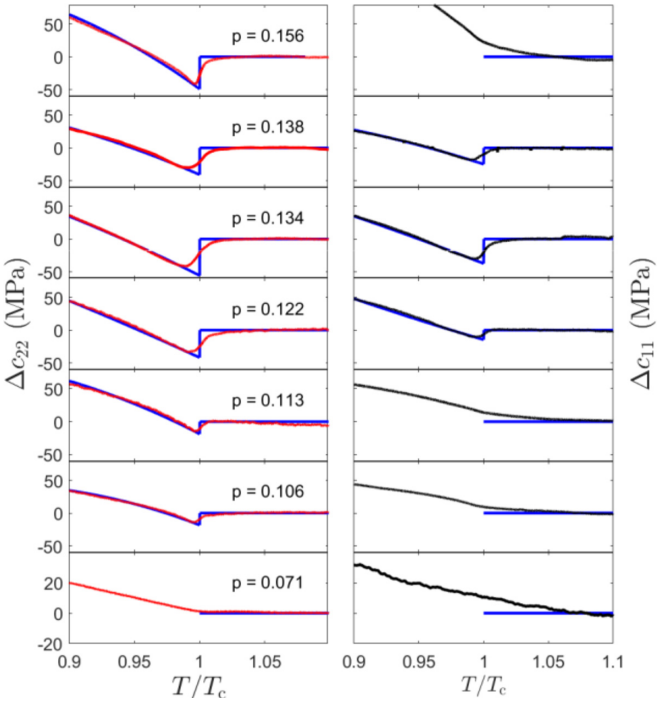

FIG. 1. Superconducting contribution to $c_{22}(T)$ (red, left column) and $c_{11}(T)$ (black, right column) near T_c as a function of doping in YBCO. A fit based on a thermodynamic model [27] is shown in blue. It is used to extract $\Delta c_{ii}(T_c)$, the mean-field jump-like anomaly at T_c. When no jump is observed we can extract an upper limit for $dT_c/d\epsilon_{ii}$ which depends on measurement noise level and on the amplitude of the specific heat jump at T_c. T_c is defined as the position of the mean-field anomaly in $\Delta c_{ii}(T)$. The scale is the same for all doping levels except for $p = 0.071$ where the vertical scale is reduced for clarity.

increase in anisotropy with decreasing doping level reflects the fact that the pseudogap potential enhances as the system approaches the Mott insulating state by reducing p.

The sound velocities of several detwinned YBCO samples (see Table I for characteristics) measured across their superconducting transition temperature T_c are shown in Fig. 1 [see Supplemental Material (SM) [27] for experimental details and

TABLE I. Characteristics of the YBCO samples measured in this study: the oxygen content y; the superconducting transition temperature in zero magnetic field T_c; the hole concentration (doping) p, obtained from T_c [26]. Typical $dT_c/d\epsilon_{11}$ and $dT_c/d\epsilon_{22}$ are given for each oxygen content y.

y	T_c (K)	p (holes/Cu)	$dT_c/d\epsilon_{11}$ (K)	$dT_c/d\epsilon_{22}$ (K)
6.45	34.0	0.071	0 ± 50	0 ± 50
6.48	55.8	0.095		380 ± 52
6.51	60.0	0.106	0 ± 50	440 ± 70
6.55	62.5	0.113	0 ± 50	480 ± 76
6.67	67.7	0.122	475 ± 85	720 ± 115
6.75	77.0	0.134	655 ± 135	845 ± 175
6.79	82.0	0.138	450 ± 102	560 ± 100
6.87	92.3	0.156	0 ± 50	400 ± 65
6.99	88.5	0.185		320 ± 34

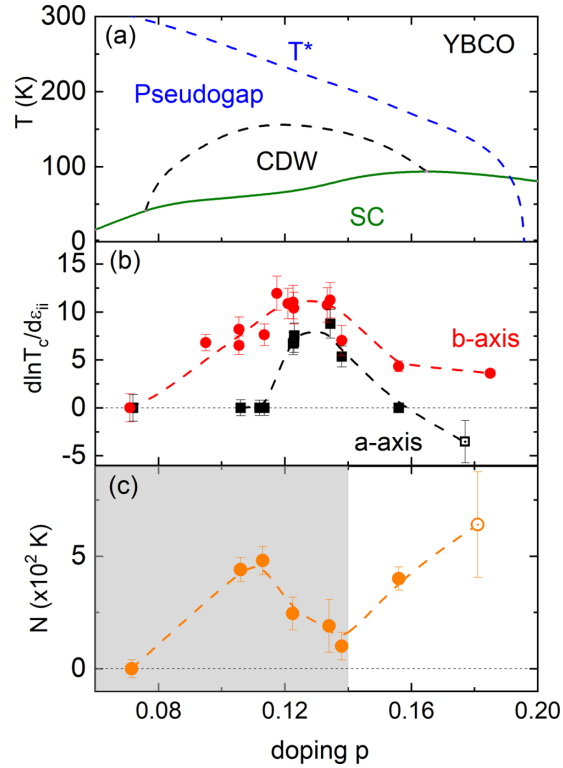

FIG. 2. (a) Temperature-doping phase diagram of YBCO in zero magnetic field. The green line is the superconducting dome, black dashed line is the dome of short-range CDW, and blue dashed line is the pseudogap onset temperature $T^\star$. (b) Doping dependence of $d\ln T_c/d\epsilon_{11}$ (black) and $d\ln T_c/d\epsilon_{22}$ (red). (c) Thermodynamic anisotropy $N = dT_c/d\epsilon_{22} - dT_c/d\epsilon_{11}$. The shaded area highlights the doping range where the anisotropy is mostly controlled by the physics of the CuO_2 planes, and consequently where comparison with the theoretical model is most relevant (see text). Dashed lines are guides to the eyes. Data from this study are shown using solid symbols [43].

additional data]. We focus on the elastic constants c_{11} and c_{22} corresponding to longitudinal modes with propagation along the a axis and b axis of the orthorhombic crystal structure of YBCO, respectively.

In Fig. 1 we show the superconducting contribution to the elastic constants, obtained after subtraction of the thermally activated anharmonic background [28]. It consists in a change of slope and curvature below T_c and a downward, mean-field jump $\Delta c_{ii}(T_c)$ at T_c. This jump is a consequence of having a term $\phi^2\epsilon_{ii}$ in the free energy that couples the strain with the superconducting order parameter ϕ [27]. Here, we focus on the magnitude of this jump $\Delta c_{ii}(T_c)$, which strongly depends on doping level and on propagation direction. In particular, an anisotropy is observed between $\Delta c_{11}(T_c)$ and $\Delta c_{22}(T_c)$ at $p \leqslant 0.11$ and $p \geqslant 0.156$: At $T = T_c$, a clear jump is observed in $\Delta c_{22}(T)$ but no jump is observed in $\Delta c_{11}(T)$. However, at the intermediate doping level the anisotropy is reduced, with a clear jump resolved in both modes. The magnitude of $\Delta c_{ii}(T_c)$ is governed by the Ehrenfest relationship [27,29–32]

$$\Delta c_{ii}(T_c) = -\frac{\Delta C_p(T_c)}{T_c}\frac{1}{V_m}\left(\frac{dT_c}{d\epsilon_{ii}}\right)^2, \quad (1)$$

with $\Delta C_p(T_c)$ the jump in the heat capacity at T_c, and V_m the molar volume. Thus, the anisotropy in Δc_{ii} implies a difference between $dT_c/d\epsilon_{ii}$ and $dT_c/d\epsilon_{22}$. We use a thermodynamic model to fit the data in Fig. 1 and to extract $\Delta c_{ii}(T_c)$ [27,33]. We then use Eq. (1), in combination with specific heat [34–36] and uniaxial pressure dependence of T_c data [21,37–42] in order to determine the amplitude and sign of $dT_c/d\epsilon_{ii}$, respectively. Since the acoustic waves are merely strain waves at finite frequency and wave vector, our method allows the extraction of $dT_c/d\epsilon_{ii}$ without actually applying static uniform strain ϵ_{ii} [27].

The resulting doping dependencies of $dT_c/d\epsilon_{11}$ and $dT_c/d\epsilon_{22}$ are shown in Fig. 2(b) and the values are reported in Table I. While both quantities show a maximum around $p \sim 0.13$, a doping-dependent anisotropy is observed. To make it clear, the thermodynamic anisotropy $N = dT_c/d\epsilon_{22} - dT_c/d\epsilon_{11}$ is plotted in Fig. 2(c). Upon decreasing the doping level, N first decreases and features a minimum for $p \sim 0.14$. Then N rises and show a maximum at $p \sim 0.11$, where $dT_c/d\epsilon_{22}$ is at least an order of magnitude larger than $|dT_c/d\epsilon_{11}| \leqslant 50$ K. Finally for $p < 0.11$, N decreases steadily as a mean-field jump is no longer resolved either in c_{11} or in c_{22} at $p = 0.071$. Thus, $N(p)$ is nonmonotonic as a function of doping, which is the main experimental result of this paper.

The behavior of $N(p)$ is to be contrasted with the monotonic increase of the orthorhombicity of YBCO with doping over similar range (see Refs. [23–25] and Fig. 4 in SM [27]). This difference in the doping trends implies that $N(p)$ is affected by an electronic property which we try to identify in the rest of the paper. Below we discuss three possible electronic scenarios.

One possible source of additional electronic anisotropy can be the short-range charge density wave (CDW) order in YBCO [10,44,45]. At face value this seems to be the case since $dT_c/d\epsilon_{22}$ and $dT_c/d\epsilon_{ii}$ are individually peaked around $p = 0.13$, which coincides with the peak in the CDW ordering temperature. However, this simply implies that the CDW contributes significantly in the symmetric channel $dT_c/d\epsilon_{22} + dT_c/d\epsilon_{11}$, which is likely due to a competition between CDW and superconductivity [46–49]. But, in the asymmetric channel $dT_c/d\epsilon_{22} - dT_c/d\epsilon_{11}$ we do not expect the CDW to be important for the following reason. The CDW state itself is either a biaxial order that preserves tetragonal symmetry [50], in which case it does not contribute to $N(p)$, or it is locally uniaxial with CDW domains running along the in-plane crystallographic axes as seen by x-ray [49,51]. However, even for the latter, the CDW will contribute to $N(p)$ only if these domains are aligned along the same direction, which is not the case in the zero strain limit probed here.

A second possible explanation could be that the system is near a second-order electronic nematic phase transition, and that $N(p)$ is proportional to the associated order parameter that presumably increases as the doping level p is reduced. In this scenario the system would have large nematic correlation length in the $(x^2 - y^2)$ symmetry channel. However, in this case one would expect the orthorhombic elastic constant to soften, as seen in the iron-based systems [52–54]. Such a softening has yet to be reported for any cuprate, while the absence of such a softening is well established for $La_{2-x}Sr_xCuO_4$ [33,55]. Moreover, electronic Raman scattering, which is a direct probe of nematicity [54], has shown the absence of nematic correlations in underdoped $Bi_2Sr_2CaCu_2O_{8+\delta}$ [20]. Consistently, dynamical mean-field studies have reported a lack of any significant nematic correlations [18], and the absence of nematic instability [56]. Consequently, while $N(p)$ is indeed an electronic anisotropy, it is unlikely to be due to the presence of a primary electronic nematic order parameter associated with a second-order phase transition, and in this sense the system is non-nematic.

The third possibility, which we explore in detail, is that $N(p)$ is governed by the opening of the pseudogap in the single-particle electronic properties. This is based on the hypothesis that the pseudogap potential varies with an external orthorhombic strain. With such an assumption we expect that varying the pseudogap strength with orthorhombic strain will also change T_c, and this process will contribute to $N(p)$. Qualitatively, in this scenario we expect that at low doping $N(p)$ vanishes with orthorhombicity for reasons of symmetry, while at high doping $N(p)$ decreases because the pseudogap strength itself reduces with doping [57]. Thus, $N(p)$ is guaranteed to have an extremum at intermediate doping. Quantitatively, our theory modeling of $N(p)$ consists of the following three steps.

First, we consider the free energy involving the superconducting order parameter ϕ and the in-plane uniform strains (u_{11}, u_{22}). To simplify the discussion we first assume a system with tetragonal symmetry. The free energy has the form

$$F = \tfrac{1}{2}a\phi^2 + \tfrac{1}{2}c_{11}u_{11}^2 + \tfrac{1}{2}c_{22}u_{22}^2 + c_{12}u_{11}u_{22} + \lambda_1(u_{11} + u_{22})\phi^2 + \tfrac{1}{2}\lambda_2(u_{11} - u_{22})^2\phi^2 + \cdots, \quad (2)$$

where the ellipsis implies terms irrelevant for the current discussion. Here, $a = a_0(T - T_c^0)$, where T_c^0 is the superconducting transition temperature in the absence of strain, $c_{11} = c_{22}$ and c_{12} are elastic constants in Voigt notation, and (λ_1, λ_2) are coupling constants. In an orthorhombic system we have $u_{11} = u_0/2 + \epsilon_{11}$, and $u_{22} = -u_0/2 + \epsilon_{22}$, where u_0 is the spontaneous orthorhombic strain, and $(\epsilon_{11}, \epsilon_{22})$ are strains that may develop in response to external stresses. Thus, to linear order in the induced strains ϵ_{ii} the transition temperature is

$$T_c(\epsilon_{ii}) = T_c^0 - \frac{2\lambda_1}{a_0}(\epsilon_{11} + \epsilon_{22}) - \frac{2\lambda_2}{a_0}u_0(\epsilon_{11} - \epsilon_{22}),$$

and from which we obtain

$$N = 4u_0\lambda_2/a_0. \quad (3)$$

Second, we deduce a microscopic expression for the parameter a_0. Since the superconducting transition is an instability in the particle-particle channel, we can write

$$a = 1/g - \frac{1}{k_B T}\sum_{\mathbf{k},\omega_n} f_{\mathbf{k}}^2 G_{\mathbf{k}}(i\omega_n)G_{-\mathbf{k}}(-i\omega_n), \quad (4)$$

where g is the pairing potential, k_B is the Boltzmann constant, $f_{\mathbf{k}}$ is a d-wave form factor, and $G_{\mathbf{k}}(i\omega_n)$ is the electron Green's function. We use the Yang-Zhang-Rice [58] type of model for the Green's function,

$$G_{\mathbf{k}}^R(\omega)^{-1} = \omega + i\Gamma_1 - \epsilon_{\mathbf{k}} - \frac{P_{\mathbf{k}}^2}{\omega + i\Gamma_2 + \xi_{\mathbf{k}}}, \quad (5)$$

which has been widely used in the literature to study the low-energy properties of the pseudogap [59–66]. Here, $\epsilon_{\mathbf{k}}$ is the electron dispersion, $\xi_{\mathbf{k}} = -\omega$ defines the line along which the electron spectral function is suppressed at a given frequency, (Γ_1, Γ_2) are inverse lifetimes, and the pseudogap potential $P_{\mathbf{k}} \equiv f_{\mathbf{k}} P_0$ is assumed to have d-wave symmetry. Once the Green's function is known, the quantity a_0 follows simply from

$$a_0 = (\partial a/\partial T)_{T=T_c^0}. \tag{6}$$

Third, we obtain a similar microscopic expression for the parameter λ_2. We consider a tetragonal system with an externally imposed orthorhombic strain $\eta \equiv u_{11} - u_{22}$. For finite η one expects mixing between A_{1g} and B_{1g} symmetries. Thus, the fourfold symmetric functions $(\epsilon_{\mathbf{k}}, \xi_{\mathbf{k}})$ develop a d-wave component, while the pseudogap potential $P_{\mathbf{k}}$ develops an s-wave component. We express these changes as $\epsilon_{\mathbf{k}} \to \tilde{\epsilon}_{\mathbf{k}} = \epsilon_{\mathbf{k}} + \alpha_1 \eta f_{\mathbf{k}}$, $\xi_{\mathbf{k}} \to \tilde{\xi}_{\mathbf{k}} = \xi_{\mathbf{k}} + \alpha_2 \eta f_{\mathbf{k}}$, and $P_{\mathbf{k}} \to \tilde{P}_{\mathbf{k}} = P_{\mathbf{k}} + \beta \eta P_0$, where (α_1, α_2) are constant energy scales and β is an important dimensionless constant capturing the change of pseudogap with *external* orthorhombic strain. From Eq. (2) we get

$$\lambda_2 = (1/2)(\partial^2 a/\partial D^2), \tag{7}$$

where the derivative

$$\frac{\partial}{\partial D} \equiv \alpha_1 f_{\mathbf{k}} \frac{\partial}{\partial \epsilon_{\mathbf{k}}} + \alpha_2 f_{\mathbf{k}} \frac{\partial}{\partial \xi_{\mathbf{k}}} + \beta P_0 \frac{\partial}{\partial P_{\mathbf{k}}}.$$

Thus, Eqs. (3)–(7) and the experimental input of u_0 obtained from diffraction data provide a means to compute the thermodynamic anisotropy N. The details of the particular microscopic model used and the technical steps for the computation of a_0 and λ_2 can be found in SM [27].

Following our earlier hypothesis, we chose the constants $(\alpha_1, \alpha_2, \beta)$ such that the derivative above is dominated by the last term which is the main pseudogap contribution. This would imply that the main contribution to $N(p)$ can be captured by

$$N(p) \approx (2/a_0)\left(\partial^2 a/\partial P_{\mathbf{k}}^2\right)\beta^2 u_0(p) P_0(p)^2. \tag{8}$$

The results of the calculation are shown in Fig. 3. Our main theoretical conclusion is that, in the presence of the pseudogap, the thermodynamic anisotropy $N(p)$ (the solid line) has a maximum around $p = 0.11$ doping, as seen in the experiments. Beyond this doping the thermodynamic anisotropy decreases even though the crystalline anisotropy, namely the spontaneous orthorhombicity $u_0(p)$, increases until around $p = 0.16$. The nonmonotonic behavior of $N(p)$ is a result of the presence of the pseudogap. This point is clearly demonstrated by the monotonic evolution of the open symbols in Fig. 3 which are obtained by setting the pseudogap to zero. In other words, the doping dependence of $N(p)$ is controlled by that of the lattice orthorhombicity $u_0(p)$ and the pseudogap potential $P_0(p)$, as expressed in Eq. (8). Thus, in Fig. 3 the initial increase of $N(p)$ for $0.065 \leqslant p \leqslant 0.11$ is driven by the increase in the orthorhombicity $u_0(p)$, with the magnitude of $N(p)$ boosted by the presence of the pseudogap, while the later decrease of $N(p)$ (the solid line) with doping beyond $p = 0.11$ is driven by a decrease of the pseudogap potential P_0 and therefore a decrease of $\lambda_2(p)$. The role of the pseudogap

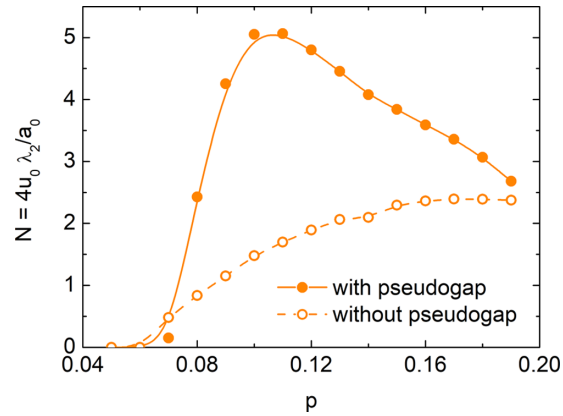

FIG. 3. Theoretical $N = 4u_0\lambda_2/a_0$ computed with $P_g \neq 0$ (solid circles) and $P_g = 0$ (open circles), using a doping dependent orthorhombicity u_0 from scattering measurements [27], and the pseudogap potential from Ref. [57]. Without the pseudogap, N increases monotonically, mimicking the doping-dependent orthorhombicity. The effect of the pseudogap is to produce a nonmonotonic N.

to enhance the in-plane electronic anisotropy has been also noted in an earlier dynamical mean-field study [56].

In the actual experiments $N(p)$ has a minimum around $p \sim 0.14$, and it increases with further hole doping, a behavior reminiscent of electrical resistivity [1] and thermal expansion [67]. In this regime the pseudogap decreases (see Fig. 2) and our model loses significance. Simultaneously, the impact of the CuO chains, whose oxygen content increases with doping, becomes increasingly significant for the anisotropy. A second possibility is that, with increasing doping the nematic correlations become stronger [20]. In addition to producing orthorhombicity, the CuO chains of YBCO also go through several structural changes in the range of oxygen content y studied here [68]. The ortho-II phase is found up to $y = 6.6$ ($p < 0.11$ or so). Then, increasing y from 6.6 to 7.0, four other CuO chain superstructures are stabilized [68]. If this sequence of CuO chain structures had an impact on the thermodynamic anisotropy N, we would expect each one of them to cause an abrupt feature in N. Instead, we observe a smooth evolution with a single broad minimum at $p \sim 0.14$. Consequently, it is unlikely that $N(p)$ is affected by these structural changes in the chains.

To conclude, using ultrasounds on YBCO we extract $dT_c/d\epsilon_{ii}$, the variation of the superconducting transition temperature T_c with in-plane strain ϵ_{ii}. We show that the in-plane thermodynamic anisotropy $N \equiv dT_c/d\epsilon_{22} - dT_c/d\epsilon_{11}$ has an intriguing doping dependence that does not follow that of the crystalline orthorhombicity. Theoretically, we show that the data are qualitatively consistent with Eq. (8) which suggests that uniaxial strain affects the pseudogap which, in turn, affects T_c.

Finally, an important *prediction* of our work is that, in the presence of substantial uniaxial strain, the pseudogap potential would vary significantly and, in particular, can lead to a visible gap opening in the nodal region. This prediction can be tested by performing angle-resolved photoemission, electronic Raman response, in-plane resistivity, and Hall measurements under uniaxial strain. Validation of the prediction

would imply that uniaxial pressure is an important tool to control the pseudogap, which is otherwise well known to be insensitive to external perturbations such as disorder, magnetic field, and hydrostatic pressure.

We thank C. Meingast, M. Civelli, M.-H. Julien, A. Sacuto, and Y. Gallais for valuable discussions. Part of this work was performed at the LNCMI, a member of the European Magnetic Field Laboratory (EMFL). Work at the LNCMI was supported by the Laboratoire d'Excellence LANEF (ANR-10-LABX-51-01), French Agence Nationale de la Recherche (ANR) Grant No. ANR-19-CE30-0019-01 (Neptun), and EUR Grant NanoX nANR-17-EURE-0009. Self-flux growth was performed at Scientific Facility Crystal Growth in Max Planck Institute for Solid State Research, Stuttgart, Germany with the support of the technical staff.

[1] Y. Ando, K. Segawa, S. Komiya, and A. N. Lavrov, Phys. Rev. Lett. **88**, 137005 (2002).
[2] Y. Sato, S. Kasahara, H. Murayama, Y. Kasahara, E.-G. Moon, T. Nishizaki, T. Loew, J. Porras, B. Keimer, T. Shibauchi, and Y. Matsuda, Nat. Phys. **13**, 1074 (2017).
[3] V. Hinkov, D. Haug, B. Fauqué, P. Bourges, Y. Sidis, A. Ivanov, C. Bernhard, C. T. Lin, and B. Keimer, Science **319**, 597 (2008).
[4] L. Mangin-Thro, Y. Li, Y. Sidis, and P. Bourges, Phys. Rev. Lett. **118**, 097003 (2017).
[5] A. J. Achkar, M. Zwiebler, C. McMahon, F. He, R. Sutarto, I. Djianto, Z. Hao, M. J. P. Gingras, M. Hücker, G. D. Gu *et al.*, Science **351**, 576 (2016).
[6] R. Daou, J. Chang, D. LeBoeuf, O. Cyr-Choiniere, F. Laliberte, N. Doiron-Leyraud, B. J. Ramshaw, R. Liang, D. A. Bonn, W. N. Hardy, and L. Taillefer, Nature (London) **463**, 519 (2010).
[7] O. Cyr-Choiniere, G. Grissonnanche, S. Badoux, J. Day, D. A. Bonn, W. N. Hardy, R. Liang, N. Doiron-Leyraud, and L. Taillefer, Phys. Rev. B **92**, 224502 (2015).
[8] M. J. Lawler, K. Fujita, J. Lee, A. R. Schmidt, Y. Kohsaka, C. K. Kim, H. Eisaki, S. Uchida, J. C. Davis, J. P. Sethna, and E.-A. Kim, Nature (London) **466**, 347 (2010).
[9] Y. Zheng, Y. Fei, K. Bu, W. Zhang, Y. Ding, X. Zhou, J. E. Hoffman, and Y. Yin, Sci. Rep. **7**, 8059 (2017).
[10] T. Wu, H. Mayaffre, S. Krämer, M. Horvatic, C. Berthier, W. N. Hardy, R. Liang, D. A. Bonn, and M.-H. Julien, Nat. Commun. **6**, 6438 (2015).
[11] K. Ishida, S. Hosoi, Y. Teramoto, T. Usui, Y. Mizukami, K. Itaka, Y. Matsuda, T. Watanabe, and T. Shibauchi, J. Phys. Soc. Jpn. **89**, 064707 (2020).
[12] J. Wu, A. T. Bollinger, X. He, and I. Božović, Nature (London) **547**, 432 (2017).
[13] L. Niea, G. Tarjus, and S. A. Kivelson, Proc. Natl. Acad. Sci. USA **111**, 7980 (2014).
[14] E. Fradkin, S. A. Kivelson, and J. M. Tranquada, Rev. Mod. Phys. **87**, 457 (2015).
[15] C. Morice, D. Chakraborty, X. Montiel, and C. Pépin, J. Phys.: Condens. Matter **30**, 295601 (2018).
[16] S. Sachdev, H. D. Scammell, M. S. Scheurer, and G. Tarnopolsky, Phys. Rev. B **99**, 054516 (2019).
[17] P. P. Orth, B. Jeevanesan, R. M. Fernandes, and J. Schmalian, npj Quantum Mater. **4**, 4 (2019).
[18] E. Gull, O. Parcollet, P. Werner, and A. J. Millis, Phys. Rev. B **80**, 245102 (2009).
[19] Y. Gallais, R. M. Fernandes, I. Paul, L. Chauvière, Y.-X. Yang, M.-A. Méasson, M. Cazayous, A. Sacuto, D. Colson, and A. Forget, Phys. Rev. Lett. **111**, 267001 (2013).
[20] N. Auvray, S. Benhabib, M. Cazayous, R. D. Zhong, J. Schneeloch, G. D. Gu, A. Forget, D. Colson, I. Paul, A. Sacuto, and Y. Gallais, Nat. Commun. **10**, 5209 (2019).
[21] O. Kraut, C. Meingast, G. Brauchle, H. Claus, A. Erb, G. Müller-Vogt, and H. Wühl, Physica C **205**, 139 (1993).
[22] V. Pasler, Ph.D. thesis, Karlsruhe University, 2000.
[23] J. D. Jörgensen, B. W. Veal, A. P. Paulikas, L. J. Nowicki, G. W. Crabtree, H. Claus, and W. K. Kwok, Phys. Rev. B **41**, 1863 (1990).
[24] H. Casalta, P. Schleger, P. Harris, B. Lebech, N. H. Andersen, R. Liang, P. Dosanjh, and W. N. Hardy, Physica C **258**, 321 (1996).
[25] Ch. Krüger, K. Conder, H. Schwer, and E. Kaldis, J. Solid State Chem. **134**, 356 (1997).
[26] R. Liang, D. A. Bonn, and W. N. Hardy, Phys. Rev. B **73**, 180505(R) (2006).
[27] See Supplemental Material at http://link.aps.org/supplemental/10.1103/PhysRevB.105.045110 for experimental details, additional data, fitting model, error bar estimation, comparison with uniaxial pressure results, and theory details.
[28] Y. P. Varshni, Phys. Rev. B **2**, 3952 (1970).
[29] L. R. Testardi, Phys. Rev. B **3**, 95 (1971).
[30] W. Rehwald, Adv. Phys. **22**, 721 (1973).
[31] A. J. Millis and K. M. Rabe, Phys. Rev. B **38**, 8908 (1988).
[32] B. Lüthi, *Physical Acoustics in the Solid State*, Springer Series for Solid-State Sciences Vol. 148 (Springer, Berlin, 2005).
[33] M. Nohara, T. Suzuki, Y. Maeno, T. Fujita, I. Tanaka, and H. Kojima, Phys. Rev. B **52**, 570 (1995).
[34] A. Junod, D. Eckert, T. Graf, G. Triscone, and J. Muller, Physica C **162-164**, 482 (1989).
[35] J. W. Loram, J. Luo, J. R. Cooper, W. Y. Liang, and J. L. Tallon, J. Phys. Chem. Solids **62**, 59 (2001).
[36] C. Marcenat, A. Demuer, K. Beauvois, B. Michon, A. Grockowiak, R. Liang, W. Hardy, D. A. Bonn, and T. Klein, Nat. Commun. **6**, 7927 (2015).
[37] C. Meingast, B. Blank, H. Bürkle, B. Obst, T. Wolf, H. Wühl, V. Selvamanickam, and K. Salama, Phys. Rev. B **41**, 11299 (1990).
[38] C. Meingast, O. Kraut, T. Wolf, H. Wühl, A. Erb, and G. Müller-Vogt, Phys. Rev Lett. **67**, 1634 (1991).
[39] U. Welp, M. Grimsditch, S. Fleshler, W. Nessler, J. Downey, G. W. Crabtree, and J. Guimpel, Phys. Rev. Lett. **69**, 2130 (1992).
[40] U. Welp, M. Grimsditch, S. Fleshier, W. Nessler, B. Veal, and G. W. Crabtree, J. Supercond. **7**, 159 (1994).
[41] H. A. Ludwig, R. Quenzel, S. I. Schlachter, F. W. Hornung, K. Grube, W. H. Fietz, and T. Wolf, J. Low Temp. Phys. **105**, 1385 (1996).

[42] M. E. Barber, H. Kim, T. Loew, M. Le Tacon, M. Minola, M. Konczykowski, B. Keimer, A. P. Mackenzie, and C. W. Hicks, arXiv:2101.02923.

[43] $dT_c/d\epsilon_{11}$ for $p = 0.18$ [open black square, Fig. 2(b)] is determined using measurements of T_c under uniaxial stress [39], converted into strain dependence of T_c (see SM [27]). We use this value to calculate N for $p \approx 0.18$ [open orange circle, Fig. 2(c)].

[44] G. Ghiringhelli, M. Le Tacon, M. Minola, S. Blanco-Canosa, C. Mazzoli, N. B. Brookes, G. M. D. Luca, A. Frano, D. G. Hawthorn, F. He *et al.*, Science **337**, 821 (2012).

[45] J. Chang, E. Blackburn, A. T. Holmes, N. B. Christensen, J. Larsen, J. Mesot, R. Liang, D. A. Bonn, W. N. Hardy, and A. Watenphul *et al.*, Nat Phys. **8**, 871 (2012).

[46] O. Cyr-Choinière, D. LeBoeuf, S. Badoux, S. Dufour-Beauséjour, D. A. Bonn, W. N. Hardy, R. Liang, D. Graf, N. Doiron-Leyraud, and L. Taillefer, Phys. Rev. B **98**, 064513 (2018).

[47] I. Vinograd, R. Zhou, H. Mayaffre, S. Kramer, R. Liang, W. N. Hardy, D. A. Bonn, and M.-H. Julien, Phys. Rev. B **100**, 094502 (2019).

[48] H.-H. Kim, S. M. Souliou, M. E. Barber, E. Lefrançois, M. Minola, M. Tortora, R. Heid, N. Nandi, R. A. Borzi, G. Garbarino, A. Bosak *et al.*, Science **362**, 1040 (2018).

[49] H.-H. Kim, E. Lefrançois, K. Kummer, R. Fumagalli, N. B. Brookes, D. Betto, S. Nakata, M. Tortora, J. Porras, T. Loew *et al.*, Phys. Rev. Lett. **126**, 037002 (2021).

[50] E. M. Forgan, E. Blackburn, A. T. Holmes, A. K. R. Briffa, J. Chang, L. Bouchenoire, S. D. Brown, R. Liang, D. Bonn, W. N. Hardy *et al.*, Nat. Commun. **6**, 10064 (2015).

[51] R. Comin, R. Sutarto, E. H. da Silva Neto, L. Chauviere, R. Liang, W. N. Hardy, D. A. Bonn, F. He, G. A. Sawatzky, and A. Damascelli, Science **347**, 1335 (2015).

[52] M. Yoshizawa and S. Simayi, Mod. Phys. Lett. **26**, 1230011 (2012).

[53] A. E. Böhmer, P. Burger, F. Hardy, T. Wolf, P. Schweiss, R. Fromknecht, M. Reinecker, W. Schranz, and C. Meingast, Phys. Rev. Lett. **112**, 047001 (2014).

[54] Y. Gallais and I. Paul, C. R. Phys. **17**, 113 (2016).

[55] M. Frachet, S. Benhabib, I. Vinograd, S.-F. Wu, B. Vignolle, H. Mayaffre, S. Krämer, T. Kurosawa, N. Momono, M. Oda, J. Chang, C. Proust, M.-H. Julien, and D. LeBoeuf, Phys. Rev. B **103**, 115133 (2021).

[56] S. Okamoto, D. Sénéchal, M. Civelli, and A.-M. S. Tremblay, Phys. Rev. B **82**, 180511(R) (2010).

[57] J. Tallon and J. Loram, Physica C **349**, 53 (2001).

[58] K.-Y. Yang, T. M. Rice, and F.-C. Zhang, Phys. Rev. B **73**, 174501 (2006).

[59] B. Kyung, S. S. Kancharla, D. Sénéchal, A.-M. S. Tremblay, M. Civelli, and G. Kotliar, Phys. Rev. B **73**, 165114 (2006).

[60] T. D. Stanescu and G. Kotliar, Phys. Rev. B **74**, 125110 (2006).

[61] A. Liebsch and N.-H. Tong, Phys. Rev. B **80**, 165126 (2009).

[62] S. Sakai, Y. Motome, and M. Imada, Phys. Rev. Lett. **102**, 056404 (2009).

[63] S. Sakai, M. Civelli, Y. Nomura, and M. Imada, Phys. Rev. B **92**, 180503(R) (2015).

[64] W. Wu, M. S. Scheurer, S. Chatterjee, S. Sachdev, A. Georges, and M. Ferrero, Phys. Rev. X **8**, 021048 (2018).

[65] M. R. Norman, M. Randeria, H. Ding, and J. C. Campuzano, Phys. Rev. B **57**, R11093(R) (1998).

[66] M. R. Norman, A. Kanigel, M. Randeria, U. Chatterjee, and J. C. Campuzano, Phys. Rev. B **76**, 174501 (2007).

[67] P. Nagel, Ph.D. thesis, Karlsruhe University, 2001.

[68] M. V. Zimmermann, J. R. Schneider, T. Frello, N. H. Andersen, J. Madsen, M. Kall, H. F. Poulsen, R. Liang, P. Dosanjh, and W. N. Hardy, Phys. Rev. B **68**, 104515 (2003).